THE JOURNAL OF PHYSICAL CHEMISTRY B

Article

pubs.acs.org/JPCB

2-(2-Hydroxyphenyl)-benzothiazole (HBT)-Rhodamine Dyad: Acid-Switchable Absorption and Fluorescence of Excited-State Intramolecular Proton Transfer (ESIPT)

Poulomi Majumdar and Jianzhang Zhao*

State Key Laboratory of Fine Chemicals, School of Chemical Engineering, Dalian University of Technology, E-208 West Campus, 2 Ling-Gong Road, Dalian 116024, People's Republic of China

Supporting Information

ABSTRACT: Dyad was prepared by link rhodamine and excited state intramolecular proton transfer (ESIPT) chromophore 2-(2-hydroxyphenyl)-benzothiazole (HBT) using Click reaction, with the goal to switch the absorption/emission property of ESIPT chromophore. The photophysical properties of the dyad were studied with steady state and time-resolved absorption and emission spectroscopy. In the absence of acid, that is, with rhodamine is in spirolactam structure, ESIPT was observed, the enol form emission of HBT unit was observed at 404 nm in protic solvents. In aprotic solvents, emission of the keto form of HBT was observed at 543 nm. With addition of acid such as trifluoroacetic acid, the rhodamine unit transforms to the opened amide structure, intense absorption band at 554 nm developed, as well as a strong fluorescence band at 579 nm; in EtOH, the enol emission of HBT at 406 nm was not quenched by the resonance energy transfer (RET), thus, dual fluorescence was observed. In dichloromethane, however, the fluorescence of the keto form of HBT unit was completely quenched. Thus, the absorption and emission of the ESIPT chromophore were switched by a acid/base-activatable rhodamine chromophore. Such studies will add additional modulability to the ESIPT chromophores.

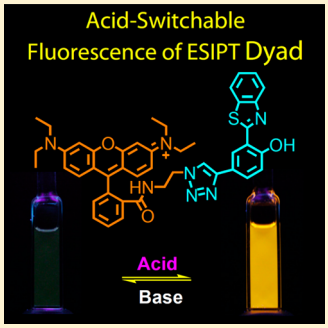

INTRODUCTION

Excited-state intramolecular proton transfer (ESIPT) have drawn considerable attention because of its unique four-level photophysical scheme, spectral sensitivity to the surrounding medium, large Stokes shifts, dual emission featured fluorescence, and so on.[1−15] These chromophores have been used in fluorescent molecular probes,[1,3−15] molecular logic gates,[4,15−17] fluorescent bioimaging,[18−26] ultraviolet stabilizers,[27] and for fundamental photophysical studies.[20,28−44]

ESIPT is phototautomerization with enol form (E) be changed to keto form (K) upon photoexcitation, by migration of a proton to the neighboring electronegative atom via intramolecular hydrogen bonding (Scheme 1). On relaxation of the keto form to the ground state, the enol form is recovered by reverse proton transfer.[45] The presence of intramolecular hydrogen bonding between the acidic proton and basic moiety is crucial. Acidic protons are usually −OH and $-NH_2$ and basic centers are =N− and carbonyl oxygen (C=O).[46,47] 2-(2-Hydroxyphenyl) benzothiazole (HBT) and 2-(2-hydroxyphenyl) benzoxazole (HBO) are well-known ESIPT dyes.[48] However, ESIPT units are rarely combined with external stimuli-responsive chromophores to attain switching effect on the spectral properties.

On the other hand, fluorescence is ideal for nondestructive tracking or analysis of chemical/biochemical substances with high sensitivity. Fluorescence as a spectral signal relay has been widely used in molecular sensors,[49−52] molecular switches,[53] pH- or enzyme-activatable photodynamic therapy (PDT) reagents,[54−56] and molecular logic gates.[57,58] Rhodamine is a well-known fluorophore that shows strong absorption and emission in visible spectral region, high fluorescent quantum yields, and high photostability. Notably, rhodamine is able to response to external stimuli, such as pH, to undergo the reversible closed rhodamine spirocyclic lactam ↔ opened amide transformation.[59−63] Accompanied with the structural transformation, the photophysical properties change substantially, that is, the switching ON and OFF of the absorption band at about 550 nm, as well as the fluorescence at about 580 nm (for rhodamine B). Hence, rhodamine derivatives have been widely used as fluorescence sensors and switches by employing this switching ON/OFF effect.[64−70] However, this unique property of rhodamine was never coupled with the ESIPT chromophore.

Concerning the aforementioned challenges, herein we prepared 2-(2-hydroxyphenyl)-benzothiazole (HBT)-rhodamine dyad (Scheme 2) to investigate the ESIPT property and fluorescence switching of the absorption and fluorescence of the ESIPT chromophore with external stimuli such as acid/base. The dyad exhibits switchable ESIPT emission property. The photophysical properties of the dyad were studied in detail

Special Issue: Photoinduced Proton Transfer in Chemistry and Biology Symposium

Received: July 9, 2014
Revised: September 10, 2014

   dx.doi.org/10.1021/jp5068507 | J. Phys. Chem. B XXXX, XXX, XXX−XXX

Scheme 1. Schematic Representation of the Four Levels ESIPT Photocycle for RH-HBT Dyad

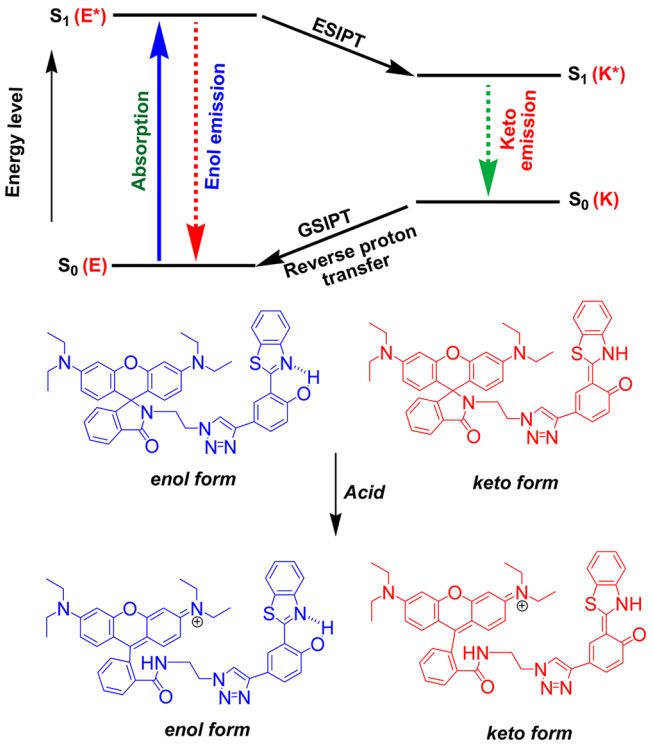

with steady state and time-resolved spectroscopy, as well as DFT/TDDFT computations.

EXPERIMENTAL SECTION

Materials and Equipment. All the chemicals are analytically pure and were used as received. Solvents were dried and distilled prior to use. ^{1}H and ^{13}C NMR spectra were recorded on a Bruker 400/500 MHz spectrophotometer ($CDCl_3$ as solvent, TMS as standard for which δ = 0.00 ppm). High resolution mass spectra (HRMS) were determined with ESI-Q-TOF MS spectrometer. Fluorescence spectra were recorded on a RF-5301PC spectrofluorometer (Shimadzu, Japan). Fluorescence quantum yields were measured with 5,10,15,20-tetraphenylporphyrin (TPP; Φ_F = 11% in toluene) and 2,6-diiodo-1,3,5,7-tetramethyl-8-phenyl-4,4-difluoroboradiazaindacene (Φ_F = 2.7% in MeCN) as standard. Fluorescence lifetimes were measured with OB920 luminescence lifetime spectrometer (Edinburgh, U.K.). Absorption spectra were recorded on an Agilent 8453A UV−vis spectrophotometer (U.S.A.).

Synthesis and Characterization. 5-Ethynyl-2-hydroxybenzaldehyde (**1**),[71] and 2-(5′-ethynyl-2′-hydroxyphenyl)-benzothiazole (**HBT**)[72,73] were synthesized according to the literature methods.

*Synthesis of Rhodamine Spirolactam (**RH**).* Under an Ar atmosphere, to a stirred solution of rhodamine B (402 mg, 0.84 mmol) in 1,2-dichloroethane (10 mL), 2-azidoethanamine (217 mg, 2.52 mmol) was added through syringe at 0 °C. To this reaction mixture phosphorus oxychloride (0.3 mL, 3 mmol) was added dropwise. The mixture was stirred at 0 °C for 15 min, heated at 85 °C for 5 h, and then stirred at 25 °C for 24 h. The solution was diluted with dichloromethane (20 mL) and acidified with 2 M HCl (30 mL). The organic layer was washed with additional 2 M HCl (2 × 30 mL), 2 M NaOH (3 × 30 mL) and brine (30 mL). The organic layer was dried over Na_2SO_4 and the solvent was evaporated under reduced pressure. The product was purified by column chromatography (silica gel, petroleum ether/EtOAc = 3:1, v/v) to give a light pink solid **RH**. Yield: 230.0 mg (53.6%); mp 186−188 °C. For the molecular structure verification with ^{1}H NMR and MS spectra, please refer to the Supporting Information.

*Synthesis of Compound **RH-HBT**.* Under an Ar atmosphere, to a stirred solution of **RH** (51.0 mg, 0.1 mmol) and **HBT** (25 mg, 0.1 mmol) in THF (10 mL), one drop of TEA was added, and the reaction mixture was stirred for 5 min at RT. Then $CuSO_4{\cdot}5H_2O$ (13 mg) in water (4 mL) and sodium ascorbate (28 mg) in water (4 mL) was added through syringe consecutively. The mixture was stirred at 30 °C for 12 h. The progress of the reaction was monitored by TLC. The reaction mixture was extracted with CH_2Cl_2. The organic layer

Scheme 2. Synthesis of HBT, HBT-1, RH, and RH-HBT[a]

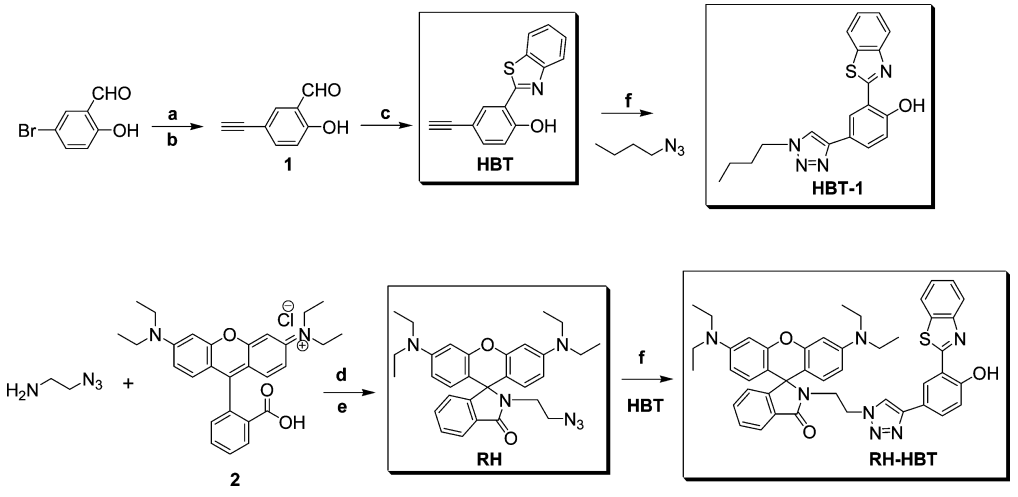

[a]Reagents and conditions: (a) Ar, ethynyltrimethylsilane, $PdCl_2(PPh_3)_2$, PPh_3, CuI, NEt_3, 80 °C, reflux, 5 h. (b) $(n\text{-Bu})_4NF$/THF, room temperature. (c) 2-Aminothiophenol, MeOH, room temperature, 12 h. (d) Under Ar, 1,2-dichloroethane, $POCl_3$, 85 °C, reflux, 4 h. (e) Under Ar, 1,2-dichloroethane, rhodamine B acid chloride, room temperature, 24 h. (f) Ar, THF, Et_3N (one drop), $CuSO_4{\cdot}5H_2O$, sodium ascorbate, 30 °C, 12 h.

dx.doi.org/10.1021/jp5068507 | J. Phys. Chem. B XXXX, XXX, XXX−XXX

was washed with brine (30 mL), dried over Na_2SO_4 and evaporated in vacuum. The product was purified by column chromatography (silica gel, petroleum ether/EtOAc = 1:1, v/v) to give **RH-HBT** as a light pink solid. Yield: 55.0 mg, 72.4%; mp 165−167 °C. For the molecular structure verification with ^{1}H NMR and MS spectra, please refer to the Supporting Information.

Synthesis of Compound ***HBT-1***. Under an Ar atmosphere, to a stirred solution of 1-azidobutane (10 mg, 0.1 mmol) and **HBT** (25 mg, 0.1 mmol) in THF (10 mL), one drop of TEA was added, and the reaction mixture was stirred for 5 min at RT. Then $CuSO_4{\cdot}5H_2O$ (13 mg) in water (4 mL) and sodium ascorbate (28 mg) in water (4 mL) was added through syringe, consecutively and allowed to stir at 30 °C for 12 h. The progress of the reaction was monitored by TLC. The reaction mixture was extracted with CH_2Cl_2. The organic layer was washed with brine (30 mL), dried over Na_2SO_4, and evaporated in vacuum. The product was purified by column chromatography (silica gel, petroleum ether/EtOAc = 1:1, v/v) to give a 25.0 mg off-white solid **HBT-1**. Yield: 71.4%; mp 173−175 °C. For the molecular structure verification with ^{1}H NMR and MS spectra, please refer to the Supporting Information.

DFT Calculations. The geometries of the compounds were optimized using density functional theory (DFT) with B3LYP functional and 6-31G(d) basis set. There are no imaginary frequencies for all optimized structures. Time-dependent DFT (TDDFT) was used for the calculation of the electronic spectra (UV−vis absorption and fluorescence emission) of the compounds. The steady-state UV−vis absorption of the organic dyes was calculated with the optimized S_0 state geometry. The fluorescence of the compounds was calculated with the optimized S_1 state geometry. All these calculations were performed with Gaussian 09W.[74]

RESULTS AND DISCUSSION

Design and Synthesis of the Dyads. Our approach to switch the absorption/emission feature of an ESIPT chromophore is to link 2-(2-hydroxyphenyl)-benzothiazole (HBT) with rhodamine via triazole unit (Scheme 2). Thus, **RH-HBT** (Scheme 2) was obtained, which is expected to show fluorescence switch on/off effect upon addition of acid/base. Reaction of 2-azidoethanamine with commercially available rhodamine B formed the light pink color rhodamine spirocyclic lactam **RH** (Scheme 2). The ethynylated HBT unit was obtained from 5-bromosalicylaldehyde through Sonogashira cross-coupling reactions. 2-(2-hydroxyphenyl)-benzothiazole (**HBT**) analogue **HBT-1** was obtained through click reaction of **HBT** and used as reference ESIPT compound. All the compounds were obtained in moderate to satisfactory yields.

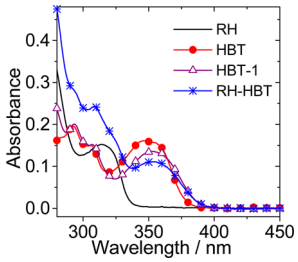

Figure 1. UV−vis absorption spectra of **RH**, **HBT**, **HBT-1**, and **RH-HBT** in dichloromethane; $c = 1.0 \times 10^{-5}$ M; 20 °C.

Scheme 3. Molecular Structures of Conformers of RH-HBT

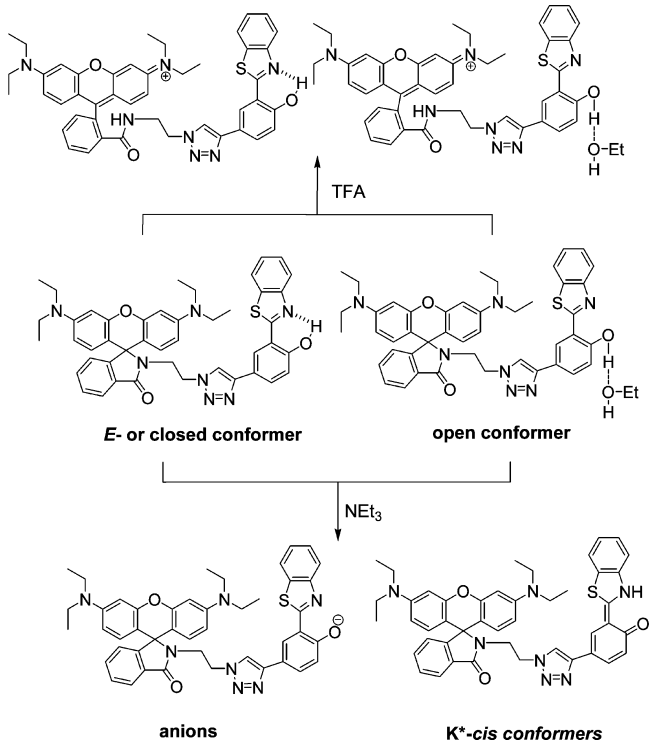

The molecular structures were fully characterized by ^{1}H NMR, ^{13}C NMR, and HRMS (see Supporting Information).

UV−Vis Absorption and Fluorescence Spectra. The absorption spectra of **HBT**, **HBT-1**, and **RH-HBT** were studied (Figures 1 and S11). These compounds exhibit absorption bands at about 290−300 nm and about 343−360 nm. The low energy absorption band are due to a $\pi-\pi^*$ transition, which is assigned to the respective closed conformer or the E-form (Schemes 3 and S1) of HBT moieties. The absorption band at about 300 nm is probably due to neutral/unsolvated open conformer of **HBT**, **HBT-1**, and **RH-HBT**. The absorption maxima are negligibly sensitive to solvent polarity,[75−78] suggesting the presence of a weak influence of inter- and intramolecular hydrogen bonding on the absorption spectra and the absence of proton transfer (PT) processes in the HBT at the ground state (S_0).[79−82] In polar protic solvent, such as methanol or ethanol, **HBT** exhibited one weak low energy band at about 400 nm (Scheme S1, open conformer **IV**).[79]

The fluorescence emission spectra and quantum yield of **HBT**, **HBT-1**, and **RH-HBT** in different polar and non polar solvents are summarized in (Table 1). In **RH-HBT** dual emissions from the enol and keto forms were observed in dichloromethane, ethyl acetate, tetrahydrofuran, methanol, and ethanol (Figure 2), the enol tautomer gives emission at shorter wavelength and the keto tautomer gives emission at longer wavelength (the fluorescence quantum yields were presented in Table S1).[82] **RH-HBT** also exhibits ESIPT in toluene, as evidenced from the strong emission at 548 nm with large Stokes shift of about 189 nm (Figure 3a). In contrast, strong enol emission with normal Stokes shift of 56 nm was observed in protic solvent (Figure 3d) because the intramolecular hydrogen bonding (−OH···N−) needed for the ESIPT process is interrupted in this solvent. A similar trend was observed for **HBT** and **HBT-1** (Figure S12).

dx.doi.org/10.1021/jp5068507 | J. Phys. Chem. B XXXX, XXX, XXX−XXX

Table 1. Photophysical Properties of Compounds in the Presence and Absence of Acid

compd	solvents	λ_{abs}[a] (nm)	ε[b]	λ_{em}[c] (nm)	Φ_F[d] (%)	τ_F[h] (ns)
RH	toluene	311	1.50	[f]	[g]	[g]
	DCM	314	1.50	[f]	[g]	[g]
	THF	315	1.54	[f]	[g]	[g]
	EtOAc	313	1.50	[f]	[g]	[g]
	MeCN	315	1.49	[f]	[g]	[g]
	MeOH	311	1.53	[f]	[g]	[g]
	EtOH	312	1.57	[f]	[g]	[g]
HBT	toluene	349	1.59	531	18.3[d]	1.65
	DCM	347	1.60	381/528	12.5[d]	3.20
	THF	348	1.62	376/533	8.1[d]	4.62 (λ_{em} = 533)
	EtOAc	345	1.62	375/532	4.5[d]	3.76
	MeCN	343	1.59	377/530	3.1[d]	4.45
	MeOH	347	1.61	387/462	33.8[d]	3.89
	EtOH	347	1.64	386/523	7.4[d]	4.67
HBT-1	toluene	357	1.37	541	10.3[d]	0.91
	DCM	353	1.34	398/539	6.5[d]	2.35 (λ_{em} = 539)
	THF	357	1.29	390/540	9.8[d]	5.5 (λ_{em} = 540)
	EtOAc	355	1.25	390/546	3.3[d]	1.82 (λ_{em} = 546)
	MeCN	352	1.33	396/541	1.8[d]	5.96 (λ_{em}= 541 nm)
	MeOH	348	1.38	409/530	16.9[d]	0.19/4.43 (λ_{em} = 530)
	EtOH	348	1.36	405/533	15.0[d]	5.05 (λ_{em} = 533)
					4.1[e]	0.22 (λ_{em} = 405)
RH-HBT	toluene	360	1.03	548	9.5[d]	0.72
	DCM	358	1.11	394/543	8.1[d]	1.93
	THF	354	1.02	386/539	4.9[d]	4.77 (λ_{em} = 539)
	EtOAc	357	0.97	374/547	2.6[d]	1.36 (λ_{em} = 547)
	MeCN	356	1.00	540	2.0[d]	6.41 (λ_{em} = 540)
	MeOH	350	1.12	404/528	5.6[d]	0.11/4.51 (λ_{em}= 528)
	EtOH	353	1.11	404/538	4.5[d]	4.10 (λ_{em} = 538)
HBT-1 + TFA	EtOH	347	1.47	407/534	3.3[e]	2.08 (λ_{em} = 534)
						0.15 (λ_{em} = 407)
RH + TFA	EtOH	554	4.30/4.56	579	25.5[e]	2.22
RH-HBT + TFA	EtOH	352/554	1.25/2.85	406/579	13.03[e]	1.87 (λ_{em} = 579)
			1.33/3.45			0.17 (λ_{em} = 406)

[a]Maxima UV−vis absorption wavelength (c = 1.0 × 10^{-5} M, 20 °C). [b]Molar extinction coefficient at the absorption maxima. ε: 10^4 M^{-1} cm^{-1}. [c]Maxima emission wavelength (c = 1.0 × 10^{-5} M, 20 °C). [d]Fluorescence quantum yields with 5,10,15,20-tetraphenylporphyrin (TPP; Φ_F = 11% in toluene) as standard. [e]Fluorescence quantum yields with 2,6-diiodo-1,3,5,7-tetramethyl-8-phenyl-4,4-difluoroboradiazaindacene (Φ_F = 2.7% in MeCN) as the standard. [f]No fluorescence. [g]Not applicable. [h]Fluorescence lifetimes under air atmosphere (c = 1.0 × 10^{-5} M, 20 °C).

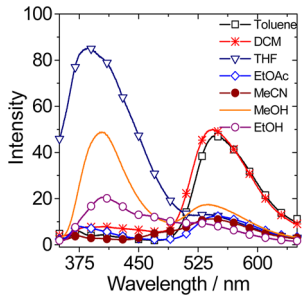

Figure 2. Fluorescence emission spectra of **RH-HBT** in different solvents; λ_{ex} = 335 nm; c = 1.0 × 10^{-5} M; 20 °C.

Effect of Acid and Base. Absorption spectra of **RH-HBT** in protic polar solvent ethanol exhibited a new absorption band at about 400 nm upon addition of base (triethylamine, TEA; Figure 4a). Similar results were observed for **HBT** and **HBT-1** (Supporting Information, Figure S14). We assume that the change is due to the formation of the respective anions of the open conformers of **HBT**, **HBT-1**, and **RH-HBT** (Schemes 3 and S1). In emission spectra of **RH-HBT**, a new emission band was observed in the range of 465−485 nm (Figure 4b) on addition of TEA due to the formation of the respective anions (Scheme S1). A gradual increase in the concentration of TEA results in an isosbestic point (Figure 4a), indicating equilibrium between the spirolactam conformer (λ_{abs} = ∼343−360 nm) and its anion (λ_{abs} = ∼400 nm; Schemes 3 and S1). On the other hand, on gradual addition of acid like trifluoroacetic acid (TFA) to the **HBT-1** (Figure S13 and S14) in ethanol results in the disappearance of the band at 400 and 465−485 nm in the absorption spectra and emission spectra, respectively, due to the interruption of intermolecular hydrogen bonding between solute and solvent in polar protic solvents. A similar trend was observed for **HBT**. Due to the presence of strong intramolecular hydrogen bonding in **RH-HBT** in nonpolar solvents, addition of base or acid has no effect on the absorption spectra/emission spectra in nonpolar solvents.

For **RH-HBT**, absorption bands at 312 and 353 nm were observed in ethanol, respectively, without any absorption band in the visible region (Figure 5). Upon addition of 5000 equiv of trifluoroacetic acid (TFA), a new strong visible absorption band at 554 nm developed due to the formation of the open-ring

dx.doi.org/10.1021/jp5068507 | J. Phys. Chem. B XXXX, XXX, XXX−XXX

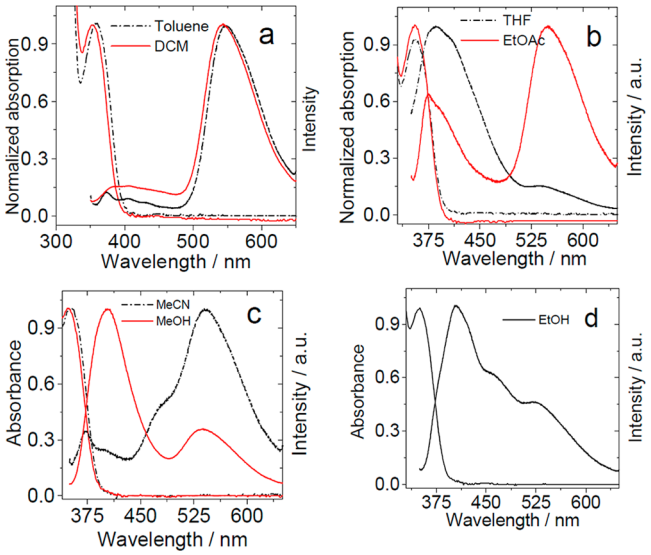

Figure 3. Normalized absorption and fluorescence spectra of **RH-HBT** in different solvents: (a) $PhCH_3$ and DCM; (b) THF and EtOAc; (c) MeCN and MeOH; (d) EtOH (c = 1.0 × 10^{-5} M); λ_{ex} = 360 nm; 20 °C.

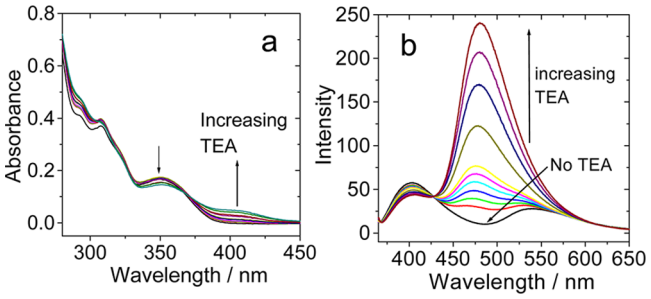

Figure 4. (a) UV−vis absorption spectra of **RH-HBT** in the presence of triethylamine (TEA). (b) Fluorescence emission spectra of **RH-HBT** in the presence of TEA; λ_{ex} = 360 nm; c = 1.0 × 10^{-5} M in ethanol; 20 °C.

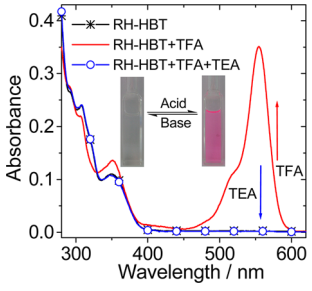

Figure 5. UV−vis absorption spectra of **RH-HBT**, **RH-HBT** + TFA (5000 equiv and 60 min standing time), **RH-HBT** + TFA (5000 equiv) + **TEA** (20 μL); c = 1.0 × 10^{-5} M in EtOH; 20 °C.

amide form of rhodamine B (**RH′** and **RH-HBT′**) from closed spirocyclic lactam form (**RH** and **RH-HBT**), correspondingly the color of the solution changed from colorless to pink (Figure 5). The sequential addition of the base such as TEA regenerates the spirocyclic lactam form of rhodamine (Figure 5), and the pink solution turns to colorless. Thus, the absorption of **RH** and **RH-HBT** in visible region can be switched ON and OFF by the spirocyclic lactam ↔ opened amide transformation of the rhodamine moiety.

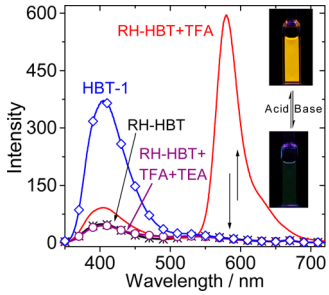

Figure 6. Fluorescence emission spectra of **HBT-1**, **RH-HBT**, **RH-HBT** + TFA (5000 equiv and 60 min standing time), and **RH-HBT** + TFA (5000 equiv) + TEA (pure 20 μL; λ_{ex} = 335 nm, where both **HBT-1** and **RH-HBT** + TFA solution give same absorbance); c = 1.0 × 10^{-5} M in EtOH; 20 °C.

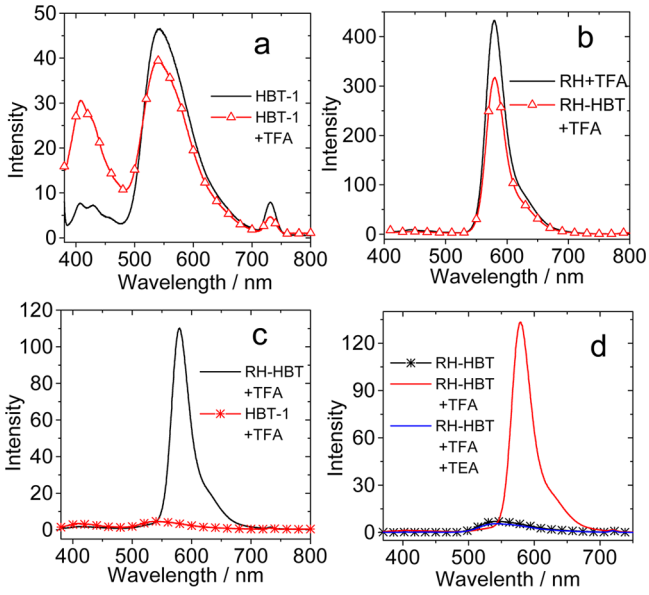

Figure 7. Fluorescence spectra of the compounds in CH_2Cl_2. (a) **HBT-1** and **HBT-1** + TFA (10000 equiv; λ_{ex} = 367 nm); (b) **RH** + TFA (10000 equiv) and **RH-HBT** + TFA (10000 equiv; λ_{ex} = 398 nm); (c) **HBT-1** + TFA (10000 equiv) and **RH-HBT** + TFA (10000 equiv; λ_{ex} = 367 nm); and (d) **RH-HBT**, **RH-HBT** + TFA (10000 equiv) and **RH-HBT** + TFA + TEA (λ_{ex} = 360 nm). In each figure, the solution of the two sample give same absorbance at the excitation wavelength so that the fluorescence emission intensity can be compared; c = 1.0 × 10^{-5} M in CH_2Cl_2; 20 °C.

The reversible switching of fluorescence emission of the dyads upon addition of acid and base were investigated (Figure 6). Initially, **RH-HBT** dyads exhibits an emission band at 404 nm (Figure 6b) due to the emission of the respective enol-form. But on addition of TFA, **RH-HBT** displayed an additional distinct strong emission band at ∼579 nm (Figure 6) due to the open-ring amide form. These bands can be switched OFF by addition of base, such as TEA (Figure 6).

HBT-1 alone in the presence of TFA does not show such switching effect. Thus, the emission of **RH-HBT** at 579 nm in the presence of TFA is due to the open-ring amide form of the rhodamine unit. Interestingly, dual emission was observed for **RH-HBT** in the presence of TFA (Figure 6), that is, the enol form emission of the HBT moiety and the rhodamine emission in **RH-HBT** were observed simultaneously (Figure 7). The nonefficient FRET may be due to the poor overlap of the emission of HBT and the absorption of rhodamine moiety. The

dx.doi.org/10.1021/jp5068507 | J. Phys. Chem. B XXXX, XXX, XXX−XXX

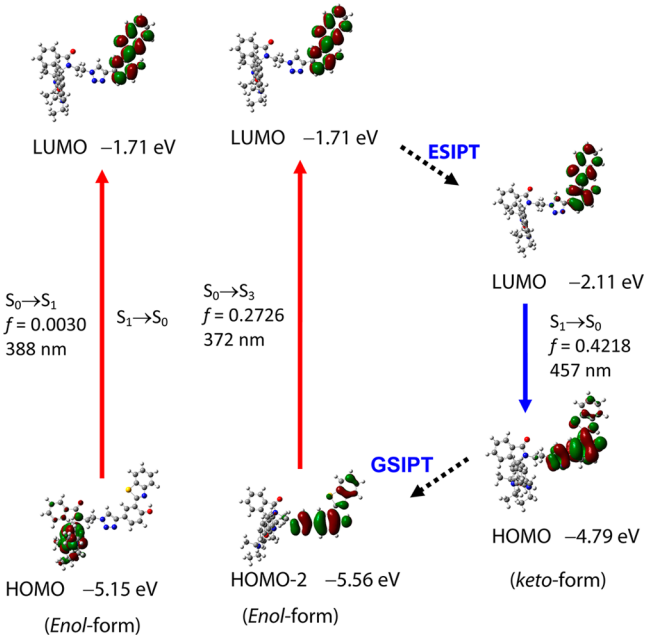

Figure 8. Selected frontier molecular orbitals involved in the vertical excitation and the singlet excited state (S_1) (both enol form and keto form were calculated) of **RH-HBT** in closed form in toluene. The calculations are based on the optimized ground state geometry (S_0 state, excitation) and exited state geometry (S_1 state, emission) at the B3LYP/6-31G(d) level using Gaussian 09W.

Table 2. Selected Electronic Excitation Energies (eV) and Corresponding Oscillator Strengths (*f*), Main Configurations, and CI Coefficients of the Low-Lying Electronic Excited States of the Closed RH-HBT Calculated by TDDFT//B3LYP/6-31g(d) Based on the DFT//B3LYP/6-31g(d) Optimized Ground State Geometries (for the UV-Vis Absorption, i.e., Excitation) and Optimized S_1 State Geometry (for the Fluorescence Emission)

	electronic transition	energy[a] (eV/nm)	*f*[b]	composition[c]	CI[d]
UV−vis	$S_0 \rightarrow S_1$	3.20/388	0.0030	H → L	0.7051
	$S_0 \rightarrow S_2$	3.33/373	0.0258	H−2 → L	0.1970
				H−1 → L	0.6777
	$S_0 \rightarrow S_3$	3.33/372	0.2726	H−2 → L	0.6682
				H−1 → L	0.2006
FL(*enol*)	$S_1 \rightarrow S_0$	3.20/388	0.0030	H → L	0.7050
FL(*keto*)	$S_1 \rightarrow S_0$	2.74/457	0.4218	H → L	0.7027

[a]Only the selected low-lying excited states are presented. [b]Oscillator strengths. [c]Only the main configurations are presented. [d]The CI coefficients are in absolute values. H, L, and FL stands for HOMO, LUMO, and fluorescence, respectively.

emission of **HBT-1** was quenched in **RH-HBT** (Figure 6), probably due to the electron transfer. In a simplified consideration by assuming that the electron transfer is the main cause of the quenching, the rate constant (k_{ET}) for the electron-transfer reaction was estimated with the following equation as to be $k_{ET} = 1.6\times 10^{10}\ s^{-1}$ (eq 1).[83]

$$k_{ET} = \left[\frac{\Phi_{F(HBT\text{-}1)}}{\Phi_{F(RH\text{-}HBT)}}\right]/\tau(HBT\text{-}1) \quad (1)$$

The spectral changes upon addition of TFA in CH_2Cl_2 were also studied (Figure 7). In DCM HBT-1 shows substantial keto emission. Upon addition of TFA, the keto emission does not change substantially. The enol form emission was enhanced (Figure 7a). For **RH-HBT**, strong emission band at 579 nm was observed upon addition of TFA, which is drastically different from the weak emission of **RH-HBT** in the absence of TFA. The emission of **RH-HBT** + TFA can be assigned to the rhodamine moiety. This new emission band upon addition of TFA was switched off by addition of base such as TEA (Figure 7d). Interestingly, the keto emission of HBT moiety was quenched in **RH-HBT** + TFA, which is different from the experiments in EtOH, for which the enol-emission band was not quenched (Figure 6). The efficient FRET in **RH-HBT** + TFA in DCM may be due to the better match of the keto emission of HBT moiety and the absorption band of rhodamine moiety. Thus, by selection of different solvents, the emission of the ESIPT chromophore is able to be either quenched or unaltered. It should be noted that there are two possibilities for this result, that is, either the ESIPT was inhibited by FRET, or ESIPT does occur, but the emission of the keto form was quenched by FRET. Considering that the ESIPT and the FRET may occur on the same time scale (ps), a competing ESIPT and FRET is plausible.[2] To the best of our knowledge, the ESIPT chromophore was rarely switched with a covalently attached external stimuli-activatable chromophore.

The cyclic spirolactam → open amide transformation of the rhodamine moiety in the dyads is found with slow kinetics. Although rhodamine has been intensively used in fluorescent molecular sensors by employing the closed spirocyclic lactam ↔ open amide form transformation, the kinetic of the closed lactam structure ↔ open amide structure was rarely studied. The kinetics of the closed lactam structure ↔ open amide structure transformation of **RH-HBT** at 554 nm upon addition of TFA were studied (Figure S17). Slow kinetics were observed for all the rhodamine-containing compounds. For **RH** and **RH-HBT**, the transformation rate constants are $k = (1.3 \pm 0.02) \times 10^{-3}\ min^{-1}$ and $k = (0.9 \pm 0.02) \times 10^{-3}\ min^{-1}$, respectively. Therefore, sufficient standing time was used in all the measurements in this paper. Interestingly, the reverse open amide → the cyclic spirolactam transformation of the rhodamine B moiety is much faster upon addition of base such as TEA and a few seconds is sufficient. This reaction kinetics was rarely reported. The kinetics is clearly important for applications based on the closed spiro lactam ↔ open amide transformations.

RH-HBT in its open amide form shows small Stokes shifts (ca. 25 nm; Figure S18) and high fluorescence quantum yields (Φ_F = 13.0%; Table 1), which are in stark contrast to the typical features of the conventional ESIPT dyes (Stokes shift > 100 nm).[84] Thus, acid- or base-activatable absorption and emission properties of the ESIPT chromophore HBT were achieved with **RH-HBT**. To the best of our knowledge, such a method was rarely used for switching the absorption and fluorescence of ESIPT chromophores.

DFT Calculations on the UV−Vis Absorption and Fluorescence Emission. DFT/TDDFT calculations have been used to study the photophysical properties of fluorophores.[85−97] The ground state geometries of the fluorophores was optimized with DFT method. The UV−vis absorption and the fluorescence emission of the compounds were calculated with TDDFT methods.

The ground state geometry of **HBT-1** was optimized (Figure S19). The calculated excitation wavelength for the $S_0 \rightarrow S_1$ transition is 371 nm, which is close to the experimental result

dx.doi.org/10.1021/jp5068507 | J. Phys. Chem. B XXXX, XXX, XXX−XXX

Table 3. Selected Electronic Excitation Energies (eV) and Corresponding Oscillator Strengths (f), Main Configurations, and CI Coefficients of the Low-Lying Electronic Excited States of the Opened Amide RH-HBT (after Addition of TFA) Calculated by TDDFT//B3LYP/6-31g(d) Based on the DFT//B3LYP/6-31g(d) Optimized Ground State Geometries (for the UV−Vis absorption, i.e., Excitation) and Optimized S_1 State Geometry (for the Fluorescence Emission)

	electronic transition	energy[a] (eV/nm)	f[b]	composition[c]	CI[d]
UV−vis	$S_0 \rightarrow S_1$	2.62/473	0.9816	H → L	0.7043
	$S_0 \rightarrow S_6$	3.59/345	0.1150	H−5 → L	0.6091
				H−6 → L	0.2355
	$S_0 \rightarrow S_8$	3.70/335	0.2886	H−1 → L+1	0.6046
	$S_0 \rightarrow S_{19}$	4.38/283	0.4560	H−2 → L+1	0.5476
FL(*enol*)	$S_1 \rightarrow S_0$	2.46/503	1.2383	H → L	0.7055

[a]Only the selected low-lying excited states are presented. [b]Oscillator strengths. [c]Only the main configurations are presented. [d]The CI coefficients are in absolute values. H, L, and FL stands for HOMO, LUMO, and fluorescence, respectively.

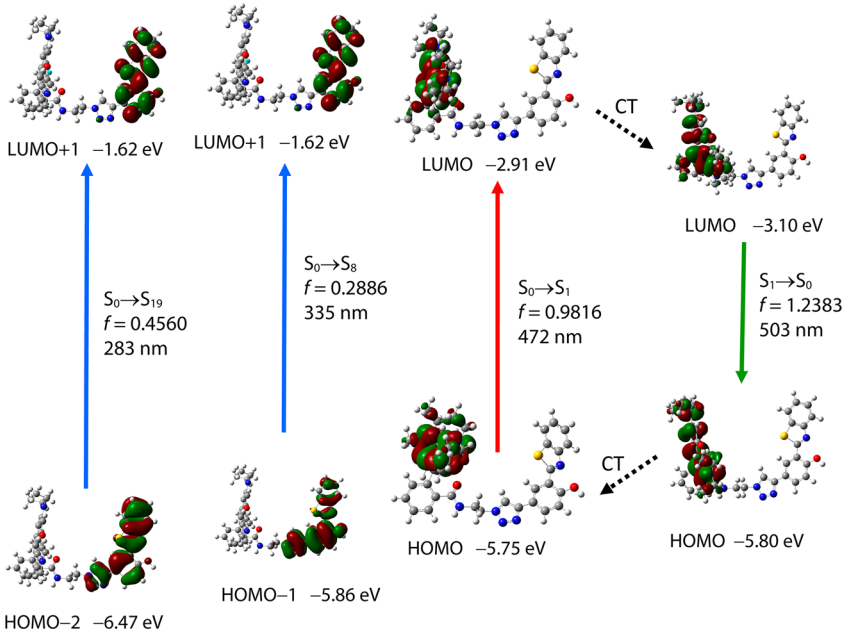

Figure 9. Selected frontier molecular orbitals involved in the vertical excitation and the singlet excited state (S_1) (both enol form and keto form were calculated) of compound **RH-HBT** open amide form in closed form in toluene. CT stands for conformation transformation. The calculations are based on the optimized ground state geometry (S_0 state, excitation) and exited state geometry (S_1 state, emission) at the B3LYP/6-31G(d)/ level using Gaussian 09W.

(357 nm, Figure 1). The electron density on the hydroxyl group decreased upon excitation, whereas the electron density on the *N* atom of benzothiazole moiety increased upon photoexcitation (Figure S19). The change in the electron density indicates that both the acidity of the hydroxyl group and the basicity of *N* atom will increase upon excitation, which coincides with the occurrence of ESIPT. The excited states geometries of both the enol and keto form of **HBT-1** were calculated (Table S2). The emission of the keto tautomer was calculated as 459 nm (the experimental results of 541 nm; Figure 2).

RH-HBT was studied with similar method (Figure 8 and Table 2). The calculated excitation wavelength for the $S_0 \rightarrow S_1$ transition is 388 nm with oscillator strength of 0.0030, which is a charge transfer state, thus can be considered as a dark state.[91] As a result, the emission of HBT may be quenched in **RH-HBT**. This postulation was supported by the experimental results (Figure 6). The low-lying allowed transition for **RH-HBT** is $S_0 \rightarrow S_3$ (372 nm) with oscillator strength of 0.2726 which is close to the experimental results of 360 nm. HOMO and LUMO have overlapped orbitals and localized on HBT unit. In **RH-HBT** also, upon photoexcitation the electron density of benzothiazole moiety increased. Due to the involvement of the frontier molecular orbitals of benzothiazole moiety, the basicity of N atom will increase upon excitation, which corresponds the occurrence of ESIPT. The calculated emission peak is at 459 nm (the experimental emission band is at 547 nm; Table 2).

Upon addition of TFA, the spirocyclic rhodamine lactam → open amide transformation, the photophysical property of the **RH-HBT** changed (Figures 5−7). With TDDFT calculation on the singlet excited state (UV−vis absorption), a new absorption band at 473 nm, with a large oscillator strength (f) of 0.9816 was observed (Table 3). HOMO → LUMO transition is involved in this absorption band, which is localized on the rhodamine open amide part (Figure 9). The calculated emission peak is at 503 nm (the experimental results of 579 nm. Figure 3). It is known that the B3LYP hybrids overestimate the excitation energy for the opened form of Rhodamine chromophore.[98] The DFT calculations indicate that the benzothiazole moiety is not involved in the frontier molecular orbitals of the absorption and emission transitions of the

dx.doi.org/10.1021/jp5068507 | J. Phys. Chem. B XXXX, XXX, XXX−XXX

rhodamine open amide part. Molecular orbitals of the **HBT** unit are involved in higher singlet excited states of **RH-HBT**, such as S_8 and S_{19} state (Figure 9 and Table 3). According to Kasha's rule, these high singlet excited states may be relaxed to the low-lying S_1 state on the rhodamine part before any fluorescence emission occurs.

CONCLUSION

In summary, 2-(2-hydroxyphenyl)-benzothiazole (HBT)-rhodamine dyad was prepared as a new excited state intramolecular proton transfer (ESIPT) chromophore, with the goal to switch the absorption/emission property of ESIPT chromophore by external stimuli, such as acid/base. The photophysical processes were studied with absorption and emission spectroscopies. The closed spirocyclic lactam form of rhodamine moiety shows no visible light absorption whereas the opened amide form of rhodamine moiety show strong absorption at 554 nm. The switching of the fluorescence of 2-(2-hydroxyphenyl)-benzothiazole (HBT)-rhodamine dyad **RH-HBT** were achieved on addition of acid/base, with which the reversible closed spirocyclic lactam form ↔ opened amide structure transformation of the rhodamine moiety takes place. The closed spirocyclic lactam form of rhodamine moiety **RH-HBT** shows the characteristics of ESIPT. Upon addition of acid in EtOH, the enol form emission band at 406 nm was not quenched by the FRET, thus dual emission band was observed. In dichloromethane, however, the keto form fluorescence emission of the HBT unit was completely quenched. Thus, the absorption and emission features of the ESIPT chromophore were successfully switched by a acid/base-activatable chromophore. These investigations will be useful to design new ESIPT chromophore as luminescent molecular probes and external stimuli-activatable fluorescent switching probes.

ASSOCIATED CONTENT

Supporting Information

^{1}H NMR, ^{13}C NMR, and HRMS spectra of **RH**, **HBT**, **HBT-1**, and **RH-HBT**. This material is available free of charge via the Internet at http://pubs.acs.org.

AUTHOR INFORMATION

Corresponding Author

*Tel.: +86 411 8498 6236. E-mail: zhaojzh@dlut.edu.cn.

Notes

The authors declare no competing financial interest.

ACKNOWLEDGMENTS

We thank the NSFC (21073028, 21273028, 21473020, and 21421005), the Royal Society (U.K.) and NSFC (China-U.K. Cost-Share Science Networks, 21011130154), Ministry of Education (SRFDP-20120041130005), Program for Changjiang Scholars and Innovative Research Team in University [IRT_13R06], the Fundamental Research Funds for the Central Universities (DUT14ZD226), and Dalian University of Technology (DUT2013TB07) for financial support.

REFERENCES

(1) Hsieh, C.-C.; Jiang, C.-M.; Chou, P.-T. Recent Experimental Advances on Excited-State Intramolecular Proton Coupled Electron Transfer Reaction. *Acc. Chem. Res.* **2010**, *43*, 1364−1374.

(2) Zhao, J.; Ji, S.; Chen, Y.; Guo, H.; Yang, P. Excited State Intramolecular Proton Transfer (ESIPT): From Principal Photophysics to the Development of New Chromophores and Applications in Fluorescent Molecular Probes and Luminescent Materials. *Phys. Chem. Chem. Phys.* **2012**, *14*, 8803−8817.

(3) Kwon, J. E.; Park, S. Y. Advanced Organic Optoelectronic Materials: Harnessing Excited-State Intramolecular Proton Transfer (ESIPT) Process. *Adv. Mater.* **2011**, *23*, 3615−3642.

(4) Wu, J.; Liu, W.; Ge, J.; Zhang, H.; Wang, P. New Sensing Mechanisms for Design of Fluorescent Chemosensors Emerging in Recent Years. *Chem. Soc. Rev.* **2011**, *40*, 3483−3495.

(5) Tang, K.-C.; Chang, M- J.; Lin, T- Y.; Pan, H- A.; Fang, T- C.; Chen, K- Y.; Hung, W- Y.; Hsu, Y- H.; Chou, P- T. Fine Tuning the Energetics of Excited-State Intramolecular Proton Transfer (ESIPT): White Light Generation in a Single ESIPT System. *J. Am. Chem. Soc.* **2011**, *133*, 17738−17745.

(6) Brewer, W. E.; Martinez, M. L.; Chou, P.-T. Mechanism of the Ground-State Reverse Proton Transfer of 2-(2-Hydroxyphenyl)-benzothiazole. *J. Phys. Chem.* **1990**, *94*, 1915−1918.

(7) Mutai, T.; Tomoda, H.; Ohkawa, T.; Yabe, Y.; Araki, K. Switching of Polymorph-Dependent ESIPT Luminescence of an Imidazo[1,2-*a*]pyridine Derivative. *Angew. Chem., Int. Ed.* **2008**, *47*, 9522−9524.

(8) Park, S.; Kwon, J. E.; Kim, S. H.; Seo, J.; Chung, K.; Park, S. Y.; Jang, D. J.; Medina, B. M.; Gierschner, J.; Park, S. Y. A White-Light-Emitting Molecule: Frustrated Energy Transfer between Constituent Emitting Centers. *J. Am. Chem. Soc.* **2009**, *131*, 14043−14049.

(9) Park, S.; Seo, J.; Kim, S. H.; Park, S. Y. Tetraphenylimidazole-Based Excited-State Intramolecular Proton-Transfer Molecules for Highly Efficient Blue Electroluminescence. *Adv. Funct. Mater.* **2008**, *18*, 726−731.

(10) Park, S.; Kwon, J. E.; Park, S. Y. Strategic Emission Color Tuning of Highly Fluorescent Imidazole-Based Excited-State Intramolecular Proton Transfer Molecules. *Phys. Chem. Chem. Phys.* **2012**, *14*, 8878−8884.

(11) Abraham, Y.; Salman, H.; Suwinska, K.; Eichen, Y. Cyclo[2]-benzimidazole: Luminescence Turn-On Sensing of Anions. *Chem. Commun.* **2011**, *47*, 6087−6089.

(12) Xu, Y.; Pang, Y. Zinc Binding-Induced Near-IR Emission from Excited-State Intramolecular Proton Transfer of a Bis(benzoxazole) Derivative. *Chem. Commun.* **2010**, *46*, 4070−4072.

(13) Kim, S. K.; Lee, D. H.; Hong, J.-I.; Yoon, J. Chemosensors for Pyrophosphate. *Acc. Chem. Res.* **2009**, *42*, 23−31.

(14) Liu, B.; Wang, H.; Wang, T.; Bao, Y.; Du, F.; Tian, J.; Li, Q.; Bai, R. A New Ratiometric ESIPT Sensor for Detection of Palladium Species in Aqueous Solution. *Chem. Commun.* **2012**, *48*, 2867−2869.

(15) Xu, Y.; Pang, Y. Zn^{2+}-Triggered Excited-State Intramolecular Proton Transfer: A Sensitive Probe with Near-Infrared Emission from Bis(benzoxazole) Derivative. *Dalton Trans.* **2011**, *40*, 1503−1509.

(16) Luxami, V.; Kumar, S. Molecular Half-Subtractor Based on 3,3′-Bis(1*H*-benzimidazolyl-2-yl)[1,1′]binaphthalenyl-2,2′-diol. *New J. Chem.* **2008**, *32*, 2074−2079.

(17) Wu, Y.; Peng, X.; Fan, J.; Gao, S.; Tian, M.; Zhao, J.; Sun, S. Fluorescence Sensing of Anions Based on Inhibition of Excited-State Intramolecular Proton Transfer. *J. Org. Chem.* **2007**, *72*, 62−70.

(18) Zamotaiev, O. M.; Postupalenko, V. Y.; Shvadchak, V. V.; Pivovarenko, V. G.; Klymchenko, A. S.; Mély, Y. Improved Hydration-Sensitive Dual-Fluorescence Labels For Monitoring Peptide−Nucleic Acid Interactions. *Bioconjugate Chem.* **2011**, *22*, 101−107.

(19) Sliwa, M.; Mouton, N.; Ruckebusch, C.; Poisson, L.; Idrissi, A.; Aloise, S.; Potier, L.; Dubois, J.; Poizat, O.; Buntinx, G. Investigation of Ultrafast Photoinduced Processes for Salicylidene Aniline in Solution and Gas Phase: Toward a General Photo-Dynamical Scheme. *Photochem. Photobiol. Sci.* **2010**, *9*, 661−669.

(20) Wang, Y.-H.; Wan, P. Excited State Intramolecular Proton Transfer (ESIPT) In Dihydroxyphenyl Anthracenes. *Photochem. Photobiol. Sci.* **2011**, *10*, 1934−1944.

(21) Brenlla, A.; Veiga, M.; Mosquera, M.; Rodriguez-Prieto, F. Fluorescence of Methylated Derivatives of Hydroxyphenylimidazopyridine. Resolution of Strongly Overlapping Spectra and a New ESIPT

Dye Showing Very Efficient Radiationless Deactivation. *Photochem. Photobiol. Sci.* **2011**, *10*, 1622−1636.
(22) Shynkar, V. V.; Klymchenko, A. S.; Kunzelmann, C.; Duportail, G.; Muller, C. D.; Demchenko, A. P.; Freyssinet, J.; Mely, Y. Fluorescent Biomembrane Probe for Ratiometric Detection of Apoptosis. *J. Am. Chem. Soc.* **2007**, *129*, 2187−2193.
(23) Kim, T.; Kang, H. J.; Han, G.; Chung, S. J.; Kim, Y. A Highly Selective Fluorescent ESIPT Probe for the Dual Specificity Phosphatase MKP-6. *Chem. Commun.* **2009**, 5895−5897.
(24) Paul, B. K.; Ray, D.; Guchhait, N. Spectral Deciphering of the Interaction Between An Intramolecular Hydrogen Bonded ESIPT Drug, 3,5-Dichlorosalicylic Acid, and A Model Transport Protein. *Phys. Chem. Chem. Phys.* **2012**, *14*, 8892−8902.
(25) Stasyuk, A. J.; Banasiewicz, M.; Cyranski, M. K.; Gryko, D. T. Imidazo[1,2-*a*]pyridines Susceptible to Excited State Intramolecular Proton Transfer: One-Pot Synthesis via an Ortoleva−King Reaction. *J. Org. Chem.* **2012**, *77*, 5552−5558.
(26) Sakai, K.-I.; Takahashi, S.; Kobayashi, A.; Akutagawa, T.; Nakamura, T.; Dosen, M.; Katoc, M.; Nagashima, U. Excited State Intramolecular Proton Transfer (ESIPT) in Six-Coordinated Zinc(II)-Quinoxaline Complexes with Ligand Hydrogen Bonds: Their Fluorescent Properties Sensitive to Axial Positions. *Dalton Trans.* **2010**, *39*, 1989−1995.
(27) Catalan, J.; Fabero, F.; Guijarro, M. S.; Claramunt, R. M.; Maria, M. D.S.; Foces-Foces, M. C.; Cano, F. H.; Elguero, J.; Sastre, R. Photoinduced Intramolecular Proton Transfer as the Mechanism of Ultraviolet Stabilizers: A Reappraisal. *J. Am. Chem. Soc.* **1990**, *112*, 747−759.
(28) Lukeman, M.; Wan, P. Excited State Intramolecular Proton Transfer (ESIPT) in 2-Phenylphenol: An Example of Proton Transfer to a Carbon of an Aromatic Ring. *Chem. Commun.* **2001**, 1004−1005.
(29) Lukeman, M.; Wan, P. A New Type of Excited-State Intramolecular Proton Transfer: Proton Transfer from Phenol OH to a Carbon Atom of an Aromatic Ring Observed for 2-Phenylphenol. *J. Am. Chem. Soc.* **2002**, *124*, 9458−9464.
(30) Lukeman, M.; Wan, P. Excited-State Intramolecular Proton Transfer in *o*-Hydroxybiaryls: A New Route to Dihydroaromatic Compounds. *J. Am. Chem. Soc.* **2003**, *125*, 1164−1165.
(31) Flegel, M.; Lukeman, M.; Huck, L.; Wan, P. Photoaddition of Water and Alcohols to the Anthracene Moiety of 9-(2′-Hydroxyphenyl)anthracene via Formal Excited State Intramolecular Proton Transfer. *J. Am. Chem. Soc.* **2004**, *126*, 7890−7897.
(32) Basaric, N.; Wan, P. Competing Excited State Intramolecular Proton Transfer Pathways from Phenol to Anthracene Moieties. *J. Org. Chem.* **2006**, *71*, 2677−2686.
(33) Basaric, N.; Wan, P. Excited State Proton Transfer (ESPT) from Phenol to Nitrogen and Carbon in (2-Hydroxyphenyl)pyridines. *Photochem. Photobiol. Sci.* **2006**, *5*, 656−664.
(34) Kim, C. H.; Joo, T. Coherent Excited State Intramolecular Proton Transfer Probed by Time-Resolved Fluorescence. *Phys. Chem. Chem. Phys.* **2009**, *11*, 10266−10269.
(35) Baiz, C. R.; Ledford, S. J.; Kubarych, K. J.; Dunietz, B. D. Beyond 7-Azaindole: Conjugation Effects on Intermolecular Double Hydrogen-Atom Transfer Reactions. *J. Phys. Chem. A* **2009**, *113*, 4862−4867.
(36) Kim, C. H.; Park, J.; Seo, J.; Park, S. Y.; Joo, T. J. Excited State Intramolecular Proton Transfer and Charge Transfer Dynamics of a 2-(2′-Hydroxyphenyl)benzoxazole Derivative in Solution. *J. Phys. Chem. A* **2010**, *114*, 5618−5629.
(37) Iijima, T.; Momotake, A.; Shinohara, Y.; Sato, T.; Nishimura, Y.; Arai, T. Excited-State Intramolecular Proton Transfer of Naphthalene-Fused 2-(2′-Hydroxyaryl)benzazole Family. *J. Phys. Chem. A* **2010**, *114*, 1603−1609.
(38) Lee, J.; Kim, C. H.; Joo, T. Active Role of Proton in Excited State Intramolecular Proton Transfer Reaction. *J. Phys. Chem. A* **2013**, *117*, 1400−1405.
(39) Chuang, W.; Hsieh, C.; Lai, C.; Lai, C.; Shih, C.; Chen, K.; Hung, W.; Hsu, Y.; Chou, P. Excited-State Intramolecular Proton Transfer Molecules Bearing *o*-Hydroxy Analogues of Green Fluorescent Protein Chromophore. *J. Org. Chem.* **2011**, *76*, 8189−8202.
(40) Stephan, J. S.; Grellmann, K. H. Photoisomerization of 2-(2′-Hydroxyphenyl) Benzoxazole. Formation and Decay of the Trans-Keto Tautomer in Dry and in Water-Containing 3-Methylpentane. *J. Phys. Chem.* **1995**, *99*, 10066−10068.
(41) Vázquez, S. R.; Rodríguez, M. C. R.; Mosquera, M.; Rodríguez-Prieto, F. Excited-State Intramolecular Proton Transfer in 2-(3′-Hydroxy-2′-pyridyl)benzoxazole. Evidence of Coupled Proton and Charge Transfer in the Excited State of Some *o*-Hydroxyarylbenzazoles. *J. Phys. Chem. A* **2007**, *111*, 1814−1826.
(42) Park, S.; Kwon, O.; Lee, Y.; Jang, D.; Park, S. Y. Imidazole-Based Excited-State Intramolecular Proton-Transfer (ESIPT) Materials: Observation of Thermally Activated Delayed Fluorescence (TDF). *J. Phys. Chem. A* **2007**, *111*, 9649−9653.
(43) Zhao, G.-J; Han, K.-L. Hydrogen Bonding in the Electronic Excited State. *Acc. Chem. Res.* **2012**, *45*, 404−413.
(44) Rios, M. A.; Rios, M. C. Ab Initio Study of the Hydrogen Bond and Proton Transfer in 2-(2′-Hydroxyphenyl)benzothiazole and 2-(2′-Hydroxyphenyl)bezimidazole. *J. Phys. Chem. A* **1998**, *102*, 1560−1567.
(45) Abou-Zied, O. K.; Jimenez, R.; Thompson, E. H. Z.; Millar, D. P.; Romesberg, F. E. Solvent-Dependent Photoinduced Tautomerization of 2-(2′-Hydroxyphenyl)benzoxazole. *J. Phys. Chem. A* **2002**, *106*, 3665−3672.
(46) Patil, V. S.; Padalkar, V. S.; Tathe, A. B.; Gupta, V. D.; Sekar, N. Synthesis, Photo-physical and DFT Studies of ESIPT Inspired Novel 2-(2′,4′-Dihydroxyphenyl) Benzimidazole, Benzoxazole and Benzothiazole. *J. Fluoresc.* **2013**, *23*, 1019−1029.
(47) Sinha, H.; Dogra, S. Ground and Excited State Prototropic Reactions in 2-(O-Hydroxyphenyl) Benzimidazole. *Chem. Phys.* **1986**, *102*, 337−347.
(48) Ikegami, M.; Arai, T. Photoinduced Intramolecular Hydrogen Atom Transfer in 2-(2-Hydroxyphenyl)benzoxazole and 2-(2-Hydroxyphenyl) Benzothiazole Studied by Laser Flash Photolysis. *J. Chem. Soc., Perkin Trans.* **2002**, *2*, 1296−1301.
(49) De Silva, A. P.; Gunaratne, H. Q. N.; Gunnlaugsson, T.; Huxley, A. J. M.; McCoy, C. P.; Rademacher, J. T.; Rice, T. E. Signaling Recognition Events with Fluorescent Sensors and Switches. *Chem. Rev.* **1997**, *97*, 1515−1566.
(50) Chen, X.; Zhou, Y.; Peng, X.; Yoon, J. Fluorescent and Colorimetric Probes for Detection of Thiols. *Chem. Soc. Rev.* **2010**, *39*, 2120−2135.
(51) Srikun, D.; Miller, E. W.; Domaille, D. W.; Chang, C. J. An ICT-Based Approach to Ratiometric Fluorescence Imaging of Hydrogen Peroxide Produced in Living Cells. *J. Am. Chem. Soc.* **2008**, *130*, 4596−4597.
(52) Zapata, F.; Caballero, A.; Espinosa, A.; Tárraga, A.; Molina, P. Triple Channel Sensing of Pb(II) Ions by a Simple Multiresponsive Ferrocene Receptor Having a 1-Deazapurine Backbone. *Org. Lett.* **2008**, *10*, 41−44.
(53) Zhang, G. X.; Zhang, D. Q.; Guo, X. F.; Zhu, D. B. A New Redox-Fluorescence Switch Based on a Triad with Tetrathiafulvalene and Anthracene Units. *Org. Lett.* **2004**, *6*, 1209−1212.
(54) Zhao, Q.; Huanga, C.; Li, F. Phosphorescent Heavy-Metal Complexes for Bioimaging. *Chem. Soc. Rev.* **2011**, *40*, 2508−2524.
(55) Gorman, A.; Killoran, J.; O'Shea, C.; Kenna, T.; Gallagher, W. M.; O'Shea, D. F. In Vitro Demonstration of the Heavy-Atom Effect for Photodynamic Therapy. *J. Am. Chem. Soc.* **2004**, *126*, 10619−10631.
(56) Tian, J.; Ding, L.; Xu, H.-J.; Shen, Z.; Ju, H.; Jia, L.; Bao, L.; Yu, J.-S. Cell-Specific and pH-Activatable Rubyrin-Loaded Nanoparticles for Highly Selective Near-Infrared Photodynamic Therapy against Cancer. *J. Am. Chem. Soc.* **2013**, *135*, 18850−18858.
(57) Erbas-Cakmak, S.; Altaná Bozdemir, O.; Cakmaka, Y.; Akkaya, E. U. Proof of Principle for a Molecular 1:2 Demultiplexer to Function as An Autonomously Switching Theranostic Device. *Chem. Sci.* **2013**, *4*, 858−862.
(58) Tian, H. Data Processing on a Unimolecular Platform. *Angew. Chem., Int. Ed.* **2010**, *49*, 4710−4712.

(59) Fan, J.; Hu, M.; Zhan, P.; Peng, X. Energy Transfer Cassettes Based on Organic Fluorophores: Construction and Applications in Ratiometric Sensing. *Chem. Soc. Rev.* **2013**, *42*, 29−43.
(60) Othman, A. B.; Lee, J. W.; Wu, J.-S.; Kim, J. S.; Abidi, R.; Thuéry, P.; Strub, J. M.; Van Dorsselaer, A.; Vicens, J. Calix[4]arene-Based, Hg^{2+}-Induced Intramolecular Fluorescence Resonance Energy Transfer Chemosensor. *J. Org. Chem.* **2007**, *72*, 7634−7640.
(61) Yuan, L.; Lin, W.; Xie, Y.; Chen, B.; Zhu, S. Single Fluorescent Probe Responds to H_2O_2, NO, and H_2O_2/NO with Three Different Sets of Fluorescence Signals. *J. Am. Chem. Soc.* **2011**, *134*, 1305−1315.
(62) Zhang, X.; Xiao, Y.; Qian, X. A Ratiometric Fluorescent Probe Based on FRET for Imaging Hg^{2+} Ions in Living Cells. *Angew. Chem., Int. Ed.* **2008**, *47*, 8025−8029.
(63) Zhang, X.; Xiao, Y.; Qian, X. Highly Efficient Energy Transfer in the Light Harvesting System Composed of Three Kinds of Boron−Dipyrromethene Derivatives. *Org. Lett.* **2008**, *10*, 29−32.
(64) Kim, H. N.; Lee, M. H.; Kim, H. J.; Kim, J. S.; Yoon, J. A New Trend in Rhodamine-Based Chemosensors: Application of Spirolactam Ring-Opening to Sensing Ions. *Chem. Soc. Rev.* **2008**, *37*, 1465−1472.
(65) Yang, Z.; She, M. Y.; Yin, B.; Cui, J. H.; Zhang, Y. Z.; Sun, W.; Li, J. L.; Shi, Z. Three Rhodamine-Based "Off−On" Chemosensors with High Selectivity and Sensitivity for Fe^{3+} Imaging in Living Cells. *J. Org. Chem.* **2012**, *77*, 1143−1147.
(66) Yang, Y. K.; Yook, K. J.; Tae, J. A Rhodamine-Based Fluorescent and Colorimetric Chemodosimeter for the Rapid Detection of Hg^{2+} Ions in Aqueous Media. *J. Am. Chem. Soc.* **2005**, *127*, 16760−16761.
(67) Ko, S. K.; Yang, Y. K.; Tae, J.; Shin, I. In Vivo Monitoring of Mercury Ions Using a Rhodamine-Based Molecular Probe. *J. Am. Chem. Soc.* **2006**, *128*, 14150−14155.
(68) Wu, J. S.; Hwang, I. C.; Kim, K. S.; Kim, J. S. Rhodamine-Based Hg^{2+}-Selective Chemodosimeter in Aqueous Solution: Fluorescent OFF−ON. *Org. Lett.* **2007**, *9*, 907−910.
(69) Zhao, Y.; Zhang, X.-B.; Han, Z.-X.; Qiao, L.; Li, C.-Y.; Jian, L.-X.; Shen, G.-L.; Yu, R.-Q. Highly Sensitive and Selective Colorimetric and Off−On Fluorescent Chemosensor for Cu^{2+} in Aqueous Solution and Living Cells. *Anal. Chem.* **2009**, *81*, 7022−7030.
(70) Xiang, Y.; Tong, A. J.; Jin, P. Y.; Ju, Y. New Fluorescent Rhodamine Hydrazone Chemosensor for Cu(II) with High Selectivity and Sensitivity. *Org. Lett.* **2006**, *8*, 2863−2866.
(71) Xu, Y.; Meng, J.; Meng, L.; Dong, Y.; Cheng, Y.; Zhu, C. A Highly Selective Fluorescence-Based Polymer Sensor Incorporating an (*R*,*R*)-Salen Moiety for Zn^{2+} Detection. *Chem.—Eur. J.* **2010**, *16*, 12898−12903.
(72) Yang, P.; Zhao, J.; Wu, W.; Yu, X.; Liu, Y. Accessing the Long-Lived Triplet Excited States in Bodipy-Conjugated 2-(2-Hydroxyphenyl) Benzothiazole/Benzoxazoles and Applications as Organic Triplet Photosensitizers for Photooxidations. *J. Org. Chem.* **2012**, *77*, 6166−6178.
(73) Ma, J.; Zhao, J.; Yang, P.; Huang, D.; Zhang, C.; Li, Q. New Excited State Intramolecular Proton Transfer (ESIPT) Dyes Based on Naphthalimide and Observation of Long-Lived Triplet Excited States. *Chem. Commun.* **2012**, *48*, 9720−9722.
(74) Frisch, M. J. et al. *Gaussian 09*, Revision A.1; Gaussian Inc.: Wallingford, CT, 2009.
(75) Singh, R. B.; Mahanta, S.; Kar, S.; Guchhait, N. Photo-Physical Properties of 1-Hydroxy-2-Naphthaldehyde: A Combined Fluorescence Spectroscopy and Quantum Chemical Calculations. *Chem. Phys.* **2007**, *331*, 373−384.
(76) Chowdhury, P.; Panja, S.; Chakravorti, S. Excited State Prototropic Activities in 2-Hydroxy 1-Naphthaldehyde. *J. Phys. Chem. A* **2003**, *107*, 83−90.
(77) Wu, K.-C.; Cheng, Y.-M.; Lin, Y.-S.; Yeh, Y.-S.; Pu, S.-C.; Hu, Y.-H.; Yu, J.-K.; Chou, P.-T. Competitive Intramolecular Hydrogen Bonding Formation and Excited-State Proton Transfer Reaction in 1-[(Diethylamino)-methyl]-2-hydroxy-3-naphthaldehyde. *Chem. Phys. Lett.* **2004**, *384*, 203−209.
(78) Mahanta, S.; Singh, R. B.; Kar, S.; Guchhait, N. Excited State Intramolecular Proton Transfer in 3-Hydroxy-2-Naphthaldehyde: A Combined Study by Absorption and Emission Spectroscopy and Quantum Chemical Calculation. *Chem. Phys.* **2006**, *324*, 742−752.
(79) Morales, A. R.; Schafer-Hales, K. J.; Yanez, C. O.; Bondar, M. V.; Przhonska, O. V.; Marcus, A. I.; Belfield, K. D. Excited State Intramolecular Proton Transfer and Photophysics of a New Fluorenyl Two-Photon Fluorescent Probe. *ChemPhysChem* **2009**, *10*, 2073−2081.
(80) Cohen, M. D.; Flavian, S. Topochemistry. Part XXV. The Absorption Spectra of Some *N*-Salicylideneanilines and Related Anils in Solution. *J. Chem. Soc. B* **1967**, 321−328.
(81) Itoh, M.; Fujiwara, Y. Transient Absorption and Two-Step Laser Excitation Fluorescence Studies of Photoisomerization in 2-(2-Hydroxyphenyl)Benzoxazole and 2-(2-Hydroxyphenyl) Benzothiazole. *J. Am. Chem. Soc.* **1985**, *107*, 1561−1565.
(82) Seo, J.; Kim, S.; Park, S. Y. Strong Solvatochromic Fluorescence From the Intramolecular Charge-Transfer State Created by Excited-State Intramolecular Proton Transfer. *J. Am. Chem. Soc.* **2004**, *126*, 11154−11155.
(83) Apperloo, J. J.; Martineau, C.; Hal, P. A.; Roncali, J.; Janssen, R. A. J. Intra- and Intermolecular Photoinduced Energy and Electron Transfer between Oligothienylenevinylenes and *N*-Methylfulleropyrrolidine. *J. Phys. Chem. A* **2002**, *106*, 21−31.
(84) Kwak, M. J.; Kim, Y. Photostable BF_2-Chelated Fluorophores Based on 2-(2′-Hydroxyphenyl)benzoxazole and 2-(2′-Hydroxyphenyl)benzothiazole. *Bull. Korean Chem. Soc.* **2009**, *30*, 2865−2866.
(85) Kowalczyk, T.; Lin, Z.; Voorhis, T. V. Fluorescence Quenching by Photoinduced Electron Transfer in the Zn^{2+}Sensor Zinpyr-1: A Computational Investigation. *J. Phys. Chem. A* **2010**, *114*, 10427−10434.
(86) Zhao, G.-J.; Liu, J.-Y.; Zhou, L.-C.; Han, K.-L. Site-Selective Photoinduced Electron Transfer from Alcoholic Solvents to the Chromophore Facilitated by Hydrogen Bonding: A New Fluorescence Quenching Mechanism. *J. Phys. Chem. B* **2007**, *111*, 8940−8945.
(87) Laurent, A. D.; Houari, Y.; Carvalho, P. H. P. R.; Neto, B.; Neto, A. D.; Jacquemin, D. ESIPT or not ESIPT? Revisiting Recent Results on 2,1,3-Benzothiadiazole under the TD-DFT Light. *RSC Adv.* **2014**, *4*, 14189−14192.
(88) Zhang, X.; Chi, L.; Ji, S.; Wu, Y.; Song, P.; Han, K.; Guo, H.; James, T. D.; Zhao, J. Rational Design of d-PeT Phenylethynylated-Carbazole Monoboronic Acid Fluorescent Sensors for the Selective Detection of α-Hydroxyl Carboxylic Acids and Monosaccharides. *J. Am. Chem. Soc.* **2009**, *131*, 17452−17463.
(89) Han, F.; Chi, L.; Liang, X.; Ji, S.; Liu, S.; Zhou, F.; Wu, Y.; Han, K.; Zhao, J.; James, T. D. 3,6-Disubstituted Carbazole-Based Bisboronic Acids with Unusual Fluorescence Transduction as Enantioselective Fluorescent Chemosensors for Tartaric Acid. *J. Org. Chem.* **2009**, *74*, 1333−1336.
(90) Zhang, X.; Wu, Y.; Ji, S.; Guo, H.; Song, P.; Han, K.; Wu, W.; Wu, W.; James, T. D.; Zhao, J. Effect of the Electron Donor/Acceptor Orientation on the Fluorescence Transduction Efficiency of the d-PET Effect of Carbazole-Based Fluorescent Boronic Acid Sensors. *J. Org. Chem.* **2010**, *75*, 2578−2588.
(91) Ji, S.; Yang, J.; Yang, Q.; Liu, S.; Chen, M.; Zhao, J. Tuning the Intramolecular Charge Transfer of Alkynylpyrenes: Effect on Photophysical Properties and Its Application in Design of OFF−ON Fluorescent Thiol Probes. *J. Org. Chem.* **2009**, *74*, 4855−4865.
(92) Guo, H.; Jing, Y.; Yuan, X.; Ji, S.; Zhao, J.; Li, X.; Kan, Y. Highly Selective Fluorescent OFF−ON Thiol Probes Based on Dyads of BODIPY and Potent Intramolecular Electron Sink 2,4-Dinitrobenzenesulfonyl Subunits. *Org. Biomol. Chem.* **2011**, *9*, 3844−3853.
(93) Shao, J.; Sun, H.; Guo, H.; Ji, S.; Zhao, J.; Wu, W.; Yuan, X.; Zhang, C.; James, T. D. A Highly Selective Red-Emitting FRET Fluorescent Molecular Probe Derived from BODIPY for the Detection of Cysteine And Homocysteine: An Experimental and Theoretical Study. *Chem. Sci.* **2012**, *3*, 1049−1061.
(94) Deng, L.; Wu, W.; Guo, H.; Zhao, J.; Ji, S.; Zhang, X.; Yuan, X.; Zhang, C. Colorimetric and Ratiometric Fluorescent Chemosensor Based on Diketopyrrolopyrrole for Selective Detection of Thiols: An

dx.doi.org/10.1021/jp5068507 | *J. Phys. Chem. B* XXXX, XXX, XXX−XXX

Experimental and Theoretical Study. *J. Org. Chem.* **2011**, *76*, 9294−9304.
(95) Zhou, F.; Shao, J.; Yang, Y.; Zhao, J.; Guo, H.; Li, X.; Ji, S.; Zhang, Z. Molecular Rotors as Fluorescent Viscosity Sensors: Molecular Design, Polarity Sensitivity, Dipole Moments Changes, Screening Solvents, and Deactivation Channel of the Excited States. *Eur. J. Org. Chem.* **2011**, 4773−4787.
(96) Ji, S.; Guo, H.; Yuan, X.; Li, X.; Ding, H.; Gao, P.; Zhao, C.; Wu, W.; Wu, W.; Zhao, J. A Highly Selective OFF-ON Red-Emitting Phosphorescent Thiol Probe with Large Stokes Shift and Long Luminescent Lifetime. *Org. Lett.* **2010**, *12*, 2876−2879.
(97) Shao, J.; Ji, S.; Li, X.; Zhao, J.; Zhou, F.; Guo, H. Thiophene-Inserted Aryl−Dicyanovinyl Compounds: The Second Generation of Fluorescent Molecular Rotors with Significantly Redshifted Emission and Large Stokes Shift. *Eur. J. Org. Chem.* **2011**, *39*, 6100−6109.
(98) Savarese, M.; Aliberti, A.; De Santo, I.; Battista, E.; Causa, F.; Netti, P. A.; Rega, N. Fluorescence Lifetimes and Quantum Yields of Rhodamine Derivatives: New Insights from Theory and Experiment. *J. Phys. Chem. A* **2012**, *116*, 7491−7497.

dx.doi.org/10.1021/jp5068507 | *J. Phys. Chem. B* XXXX, XXX, XXX−XXX